Carbothermal Reduction of Zinc Ferrite

JYH-JEN LEE, CHUN-I LIN, and HSI-KUEI CHEN

The carbothermal reduction of zinc ferrite was studied using X-ray diffractometer (XRD), wet chemical analysis, scanning electron microscope (SEM), surface area meter, and thermogravimetrical analysis (TGA) systems. Zinc ferrite was found to be decomposed to ZnO and Fe_2O_3 initially and carbothermal reduction of ZnO and Fe_2O_3 took place simultaneously. The results of the surface area measurement indicated that the surface area of the solid sample increased with reaction time. Pore volume and average pore diameter were found to increase, reach a maximum, and then decrease with reaction time. These results were explained by considering the escape of zinc vapor, the expansion of the iron oxide grain, and the sintering of the iron. A mechanism and a model were proposed to explain the reaction. The experimental results of the thermogravimetrical analysis indicated that the reaction rate can be increased by increasing either the argon flow rate or the reaction temperature. Furthermore, the reaction rate was found to increase with a decrease in either the sample height, the molar ratio of $ZnFe_2O_4$/C, the size of the carbon agglomerate, or the initial bulk density.

I. INTRODUCTION

ELECTRIC arc furnace (EAF) dust is produced during the steelmaking process. Toxic metals such as zinc, lead, cadmium, and nickel are present in the dust. These toxic materials are leached out by rain; they pollute both ground and underground water if the EAF dust is dumped into a landfill. Hence, the treatment of EAF dust emerges from the viewpoint of environmental protection. There are four technologies that can be applied to treat the dust:[1] (1) hydrometallurgical methods involving acidic or basic leaching,[2] (2) stabilizing techniques using cement and other additives,[3] (3) glassification,[4] and (4) pyrometallurgical treatment methods.[2] Acids or bases used in the hydrometallurgical method may pollute water. Stabilization and glassification are not only costly but also not environmentally friendly. Carbothermal reductions are the main reactions in the pyrometallurgical treatment methods. Zinc and lead can be recovered by this method. On the other hand, the byproduct, slag, can be used as construction material. Hence, pyrometallurgical treatment is the major method used in Taiwan.[1] Many reports on the carbothermal reduction of EAF dust or related topics are available and include the reduction of pure zinc oxide with carbon,[5–9] the reduction of pure lead oxide with carbon,[10] the reduction of zinc oxide with iron,[11] the reduction of EAF dust with coal, graphite, charcoal, or carbon monoxide,[12–16] and the reduction of EAF dust with iron.[17]

The zinc content in EAF dust is about 20 pct,[1] while zinc in the form of zinc ferrite is approximately 20 to 50 pct, with the remainder being zinc oxide.[17] Hence, carbothermal reductions of zinc ferrite and zinc oxide occur simultaneously during the process of the reduction of the dust. Unfortunately, literature on the carbothermal reduction of zinc ferrite cannot be found except in the work of Kim and Han.[18]

JYH-JEN LEE, Graduate Student, and CHUN-I LIN, Professor, are with the Department of Chemical Engineering, National Taiwan University of Science and Technology, Taipei, Taiwan 106. HSI-KUEI CHEN, Associate Professor, is with the Department of Chemical Engineering, Hwa-Hsia College of Technology and Commerce, Taipei, Taiwan 235.

Manuscript submitted September 18, 2000.

In the present work, the reaction of zinc ferrite with carbon black powder in an inert gas stream is studied. An X-ray diffractometer (XRD) and a wet chemical analysis are used to determine the variations in the composition of the solid sample with time. A scanning electron microscope (SEM) and a surface area meter are employed to monitor the change in the structure of the sample during reaction. A thermogravimetrical analysis system (TGA) is used to determine the reaction rate. A reaction mechanism and a reaction model are developed to account for the experimental results. Effort is also made to examine the effects of the following factors on the rate of reaction between zinc ferrite and carbon: argon flow rate, sample height, temperature, molar ratio of $ZnFe_2O_4$/C, size of carbon agglomerate, and initial bulk density. This study may help enhance the understanding of the reaction system.

II. THERMODYNAMIC CONSIDERATIONS

The overall reaction of the carbothermal reduction of zinc ferrite is considered to be[14]

$$ZnFe_2O_4\ (s) + 4C\ (s) = Zn\ (g) + 2Fe\ (s) + 4CO\ (g) \quad [1]$$

A formula for the standard free energy change has been rewritten as Eq. [2][19]

$$\Delta G^\circ = 867{,}500 - 829.4T \quad [2]$$

According to this equation, Reaction [1] is favorable over the range of 1073 to 1473 K.

III. EXPERIMENTAL

A. *Materials*

Argon (Yuan-Ron Gas Co., Taipei, Taiwan) with a minimum 99.995 pct purity was used. Zinc oxide of reagent grade with a purity of 99.9 pct was produced by the Cerac Chem. Co. (Milwaukee, WI). Ferric oxide (reagent grade, minimum purity 99.8 pct) was supplied by the Strem Chem. Co. (Newburyport, MA). The carbon source was carbon black powder (Strem Chem. Co., Newburyport, MA).

B. *Synthesis of Zinc Ferrite*

Zinc ferrite was synthesized in the laboratory. Zinc oxide (ZnO) and ferric oxide (Fe_2O_3) were initially dried in an oven at 378 K for 43,200 seconds and then screened separately. Grains within the range of 350 to 400 Tylor mesh were employed for synthesis. Zinc oxide and iron oxide powders with equimolar ratio were mixed in a beaker using xylene as a dispersing medium. The mixing continued until the xylene completely evaporated. The mixed sample was then dried at 378 K for 43,200 seconds. Synthesis was carried out in a box furnace. When the furnace was heated up to 1123 K and stabilized at this value, the alumina boat with 0.003 kg of mixed powder was loaded and synthesis started. After 18,000 seconds, the sample was removed and cooled by air. The synthesized product was then analyzed by an XRD to determine the amounts of the residues of ZnO and Fe_2O_3. The content of $ZnFe_2O_4$ was calculated by subtraction. Three experimental runs were performed and the average weight percentage of $ZnFe_2O_4$ was determined to be 96.84 ± 1.1 wt pct. The average size of the product powder was measured to be 62.61×10^{-6} m by a laser diffraction particle size analyzer (model SALD-2001, Shimadzu, Kyoto, Japan). The zinc ferrite thus produced was used for carbothermal reduction.

C. *Carbothermal Reduction of Zinc Ferrite*

Zinc ferrite and carbon black were dried at 378 K for 43,200 seconds. Screened carbon powder and zinc ferrite powder with a specified molar ratio were mixed in a V-type blender (model 8692, Tsutsui Rika, Tokyo, Japan) for 21,600 seconds. Finally, the mixed powder was dried at 378 K again until the weight of the sample remained constant.

A carbothermal reduction of zinc ferrite was conducted in a typical TGA, in which argon was flowing. The TGA employed was constructed by the members of this laboratory. From 0.5 to 3 g of mixed powder was placed in an alumina crucible (0.03 m in height and 0.02 m in diameter). The crucible was suspended by a quartz thread from the balance and the weight of the sample during the reaction was monitored with the help of a computer.

The reaction tube without solid sample was first heated up while argon was flowing through the tube. When a desired temperature was reached and maintained for several minutes, the reaction tube was opened and the crucible with sample was loaded. Then, the reaction tube was closed and reaction started. The pressure in the reactor was maintained at a level from 196 to 392 Pa higher than atmospheric pressure during reaction. After a predetermined time, the sample was removed from the tube and quenched by an argon stream.

The typical parameters and conditions studied are listed in Table I, in which the underlined values represent the standard conditions. In other words, when the effect of that condition is not studied, its value is held at the underlined value in that series of experiments. Eight partially reacted solid samples were analyzed using an XRD, a wet chemical analysis, an SEM, and a surface area meter.

The quantitative method for the carbothermal reduction is presented as follows.

Based on the mass balance of Reaction [1], the total moles of zinc ferrite reacted at time t, $\Delta N_{ZnFe_2O_4}$, is

$$\Delta N_{ZnFe_2O_4} = \frac{\Delta W}{MW_{Zn} + 4MW_{CO}} \quad [3]$$

Table I. Parameters and Conditions of Carbothermal Reduction of Zinc Ferrite

Parameter	Condition Value*
Ar flow rate (10^{-5} m^3 s^{-1})	0.833, 0.9, 1.25, 1.67, 2, <u>2.23</u>
Sample height (m)	0.0025, <u>0.005</u>, 0.01, 0.02
Reaction temperature (K)	1073, 1173, 1273, <u>1323</u>, 1373, 1473
Molar ratio of $ZnFe_2O_4$/C (—)	1/2, 1/4, <u>1/6</u>, 1/8
Size of carbon agglomerate (10^{-6} m)	<u>38.9</u>, 67.2, 120.9, 190.9
Average $ZnFe_2O_4$ grain size (10^{-6} m)	<u>62.6</u>
Initial bulk density (kg m^{-3})	<u>785.9</u>, 982.6, 1178.2, 1375.6

*Underlined values are standard operating variables.

where ΔW = weight loss at time t, which can be determined from TGA; MW_{Zn} = molecular weight of zinc, 65.37; and MW_{CO} = molecular weight of carbon monoxide, 28.

Hence, the conversion of zinc ferrite, $X_{ZnFe_2O_4}$, can be calculated according to following equation:

$$X_{ZnFe_2O_4} = \frac{\Delta N_{ZnFe_2O_4}}{N^{\circ}_{ZnFe_2O_4}} \quad [4]$$

where $N^{\circ}_{ZnFe_2O_4}$ = number of initial moles of zinc ferrite in solid sample, which is known.

In the actual case, there are some trace amounts of CO_2 produced, especially at low temperatures, due to the incompleteness of the Boudouard reaction, which will be discussed later, in this reaction system. Hence, the total amount of zinc ferrite reacted should be somewhat different from that calculated by Eq. [3]. However, the error thus introduced is normally negligible.

D. *Analysis by XRD*

Solid samples partially reacted under standard conditions were ground by a pestle and a mortar to fine powder for the XRD analysis. Copper K_α radiation was generated by a Rotaflex Ru-200B diffractometer (Tokyo), utilizing an acceleration voltage of 40 kV and a current of 100 mA. A diffraction angle of 10 to 90 deg was scanned at a rate of 10 deg/min.

E. *Wet Chemical Analysis*

The content of the Fe, FeO, and Fe_2O_3 in the partially reacted solid samples was determined by a redox titration method, which was performed by the China Steel Corporation (Kaohsiung, Taiwan). The potentiometer automatic titration employed was model At-200 of the Kyoto Electronic Corporation (Kyoto, Japan). The electrode used was a platinum-calomel composite one. The electronic potential was set between 450 and 600 mV. The concentration of oxidant, potassium dichromate, was 0.1 N.

F. *Analysis by SEM*

The appearance of the grains containing zinc ferrite and carbon during reaction were observed with an SEM (model S36, Cambridge, Cambridge, United Kingdom). An accelerating voltage of 20 kV was utilized for this purpose.

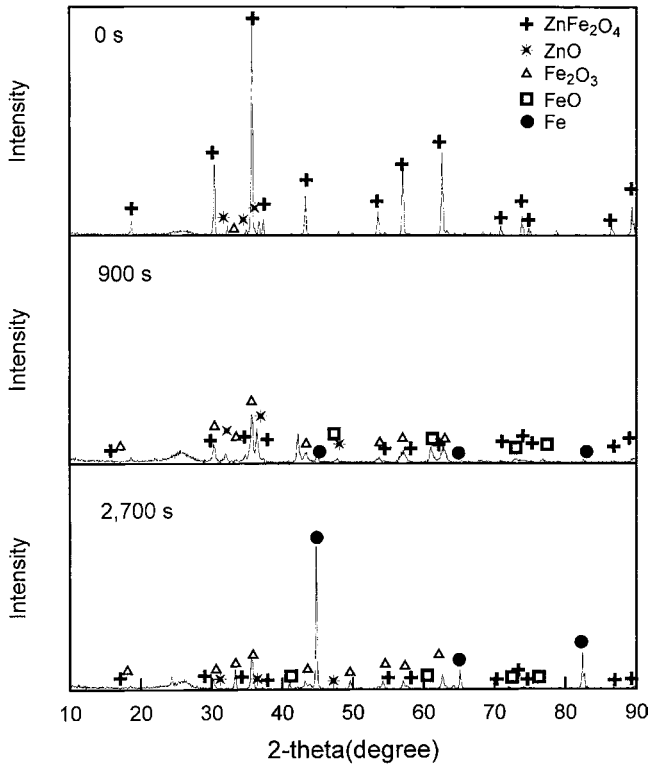

Fig. 1—XRD patterns of partially reacted solids for various reactions times. Reaction temperature = 1323 K.

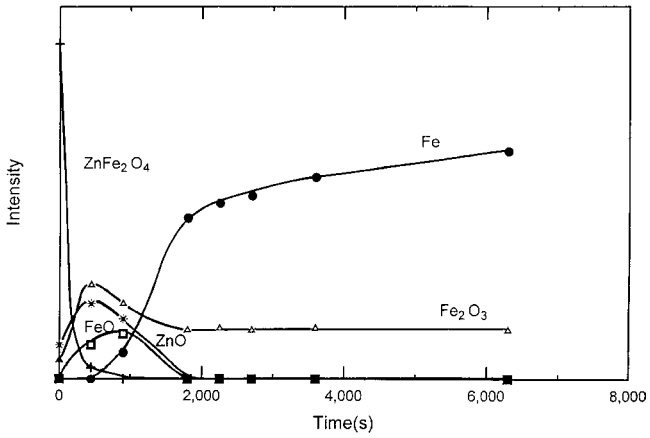

Fig. 2—Variations in the intensities of XRD peaks of $ZnFe_2O_4$, ZnO, Fe_2O_3, FeO, and Fe as a function of reaction time. Reaction temperature = 1323 K.

G. *Surface Area Measarement*

The specific surface area, specific pore volume, and average pore diameter of the solid sample were determined by a surface area meter (model ASAP 2000, Micromeritics, Norcross, GA). The specific surface area was determined by the adsorption method of Brunauer–Emmett–Teller (BET). Specific pore volume and average pore diameter were measured by the cumulative desorption method of Barreott–Joyner–Halenda (BJH). Adsorption and desorption isotherms of nitrogen were determined gravimetrically at liquid nitrogen temperature. Prior to the measurement, each sample was evacuated at 423 K for 10,800 seconds. To calculate the surface area and pore volume per sample, the specific surface area and specific pore volume thus obtained were multiplied by the weight of the solid sample.

IV. RESULTS AND DISCUSSIONS

A. *Analysis by XRD*

The XRD has been performed on the specimens reacted under standard conditions, namely, argon flow rate, 2.23×10^{-5} m^{-3} s^{-1}; sample height, 0.005 m; temperature, 1323 K; molar ratio of $ZnFe_2O_4$/C, 1/6; average $ZnFe_2O_4$ grain size, 62.6×10^{-6} m; and initial bulk density, 785.9 kg m^{-3} for various reaction times (0, 450, 900, 1800, 2200, 2700, 3600, and 6300 seconds). Three typical diffraction patterns are depicted in Figure 1. The species $ZnFe_2O_4$, ZnO, Fe_2O_3, FeO, and Fe have been found on the patterns. The peak for Fe_3O_4 is at $2\theta = 35.12$ deg, which is very close to that of $ZnFe_2O_4$, 34.98 deg. Hence, the peak of $ZnFe_2O_4$ may contain Fe_3O_4. The broad and low peaks in the range of 21 to 28 deg are that of the amorphous carbon. The peak intensities of $ZnFe_2O_4$ (34.98 deg), ZnO(36.85 deg), Fe_2O_3(33.35 deg), FeO(42.28 deg), and Fe(44.92 deg) were plotted against the reaction time, and the results are shown in Figure 2. It is observed that $ZnFe_2O_4$ disappears in a short time (about 450 seconds). Trace amounts of ZnO and Fe_2O_3 are found before the reaction and as time increases, the amount of ZnO and Fe_2O_3 increases, reaches a maximum value, and then decreases. The behavior of FeO is similar to that of Fe_2O_3, but with a time lag. The amount of Fe increases monotonically. Based on these observations, the presumption of the variation of the grains containing $ZnFe_2O_4$ can be stated as follows: $ZnFe_2O_4$ decomposes to ZnO and Fe_2O_3 in a short time at 1273 K, which was also proved by Kim and Han[18] in the range of 993 to 1113 K. The carbothermal reduction of ZnO and Fe_2O_3 takes place simultaneously from the beginning. Zinc produced from the reduction of ZnO escapes from the specimen in the gas state immediately, since no Zn is found in the diffraction patterns. The carbothermal reduction of Fe_2O_3 is a system of series reactions, the transformation order of which is normally considered to be $Fe_2O_3 \rightarrow Fe_3O_4 \rightarrow FeO \rightarrow Fe$.[20] All the components except Fe_3O_4 are observed in the XRD patterns of this study, since Fe_3O_4 is contained in the peak of $ZnFe_2O_4$, as stated earlier.

Accordingly a reaction mechanism for the overall Reaction [1] can be written as follows.

Initial stage:

$$ZnFe_2O_4\ (s) = ZnO\ (s) + Fe_2O_3\ (s) \quad [5]$$

$$3ZnFe_2O_4\ (s) + 4C\ (s) = 3Zn\ (g) + 2Fe_3O_4\ (s) + 4CO\ (g) \quad [6]$$

$$C\ (s) + [O] = CO\ (g) \quad [7]$$

Propagation stage I:

$$ZnO\ (s) + CO\ (g) = Zn\ (g) + CO_2\ (g) \quad [8]$$

$$3Fe_2O_3\ (s) + CO\ (g) = 2Fe_3O_4\ (s) + CO_2\ (g) \quad [9]$$

$$Fe_3O_4\ (s) + CO\ (g) = 3FeO\ (s) + CO_2\ (g) \quad [10]$$

$$FeO\ (s) + CO\ (g) = Fe\ (s) + CO_2\ (g) \quad [11]$$

$$C\ (s) + CO_2\ (g) = 2CO\ (g) \quad [12]$$

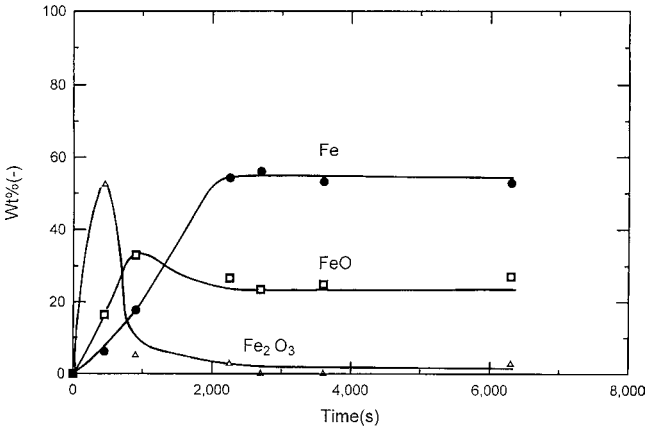

Fig. 3—Variations in the weight percentages of Fe_2O_3, FeO, and Fe as a function of reaction time. Reaction temperature = 1323 K.

Propagation stage II:

$$3Fe_2O_3\ (s) + CO\ (g) = 2Fe_3O_4\ (s) + CO_2\ (g) \quad [13]$$

$$Fe_3O_4\ (s) + CO\ (g) = 3FeO\ (s) + CO_2\ (g) \quad [14]$$

$$FeO\ (s) + CO\ (g) = Fe\ (s) + CO_2\ (g) \quad [15]$$

$$C\ (s) + CO_2\ (g) = 2CO\ (g) \quad [16]$$

Termination stage:

The reaction stops when either FeO or C is exhausted.

As mentioned earlier, $ZnFe_2O_4$ decomposes to ZnO and Fe_2O_3, as in the Reaction [5], in the range of 993 to 1323 K when the reaction starts. The other two reactions that take place in the initial stage are Reactions [6] and [7], which produce CO gas through the reaction between solids $ZnFe_2O_4$ (s) and O (s) or solid C and oxygen adsorbed on carbon, [O]. These two reactions are slow. As soon as CO gas is produced, propagation stage I starts, as do the gas/solid reactions between carbon monoxide and metal oxide (ZnO, Fe_2O_3, Fe_3O_4 or FeO) (Reactions [8] through [11]) are stimulated and carried out much faster than Reactions [6] and [7]. Hence, Reactions [6] and [7] can be neglected at this stage. In addition, the gas/solid reaction between CO (g) and O (s), the Boudouard reaction, as in Reaction [12], also proceeds. The system steps into propagation stage II as ZnO reduces completely. The reduction of iron oxides, Reactions [13] through [15], and the Boudouard reaction, Reaction [16], proceed in this stage. The system ends when either FeO or C is exhausted.

B. *Wet Chemical Analysis*

Only iron containing substances in the solid specimen were measured by wet chemical analysis; the results are depicted in Figure 3. The results of XRD (Figure 2) are qualitative measures, while those of wet chemical analysis (Figure 3) are quantitative ones. A comparison of Figures 2 and 3 shows that the shapes of the curves of Fe_2O_3, FeO, and Fe are quite similar. This similarity is considered to lend support to the results of the XRD analysis.

C. *Analysis by SEM*

Figure 4 shows the SEM micrographs of $ZnFe_2O_4$ and C. Figure 4(a) reveals that $ZnFe_2O_4$ is a dense and sphere-like

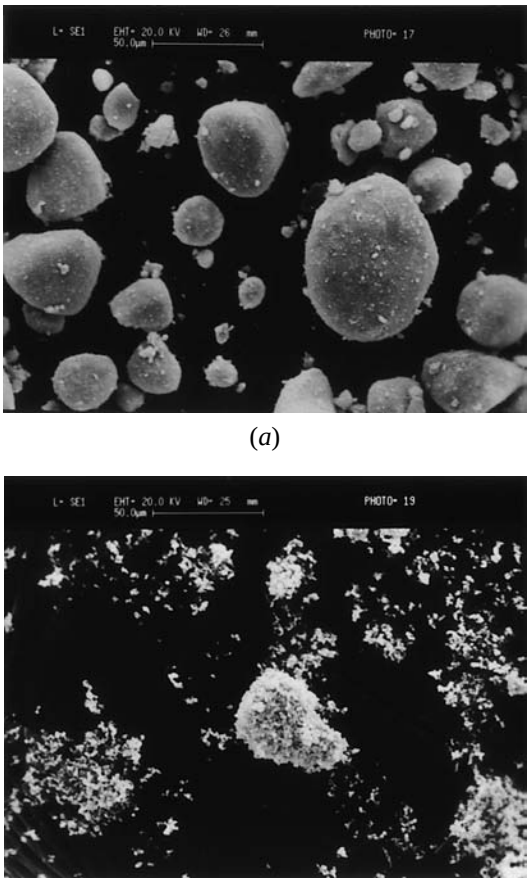

Fig. 4—SEM micrographs of (*a*) zinc ferrite and (*b*) carbon black.

grain. The grain is in the size ranging from 10×10^{-6} to 50×10^{-6} m, as compared to the 62.61×10^{-6} m determined by the laser diffraction particle size analyzer. The results of these two independent measurements are close to each other. The carbon grains in Figure 4(b) are very fine. The approximate size is 1×10^{-6} m. The grains are capable of aggregating easily to form a large agglomerate.

The SEM micrographs of unreacted and partially reacted samples with different reaction times are shown in Figure 5. The large and dense grains shown in Figure 5(a) are zinc ferrite, while the fine grains that aggregated to each other are carbon. From Figure 5(b), it can be found that many small pores are generated on the surfaces of the grains of $ZnFe_2O_4$ as the reaction proceeds (from 0 to 900 seconds). Only trace amounts of carbon grains are observed on the micrographs after 2250 seconds (Figure 5(c)). One more interesting phenomenon found from the micrographs after 2250 seconds (Figure 5(c)) is that sintering occurs on the grains containing $ZnFe_2O_4$.

D. *Surface Area Measurement*

The results of the surface area measurement, which are not shown here, indicate that the pore surface area of a sample increases with increasing time. However, the variation is not significant. The measurement of the average pore diameter of the solid sample is shown in Figure 6. The variation of the pore volume is found to be similar to that

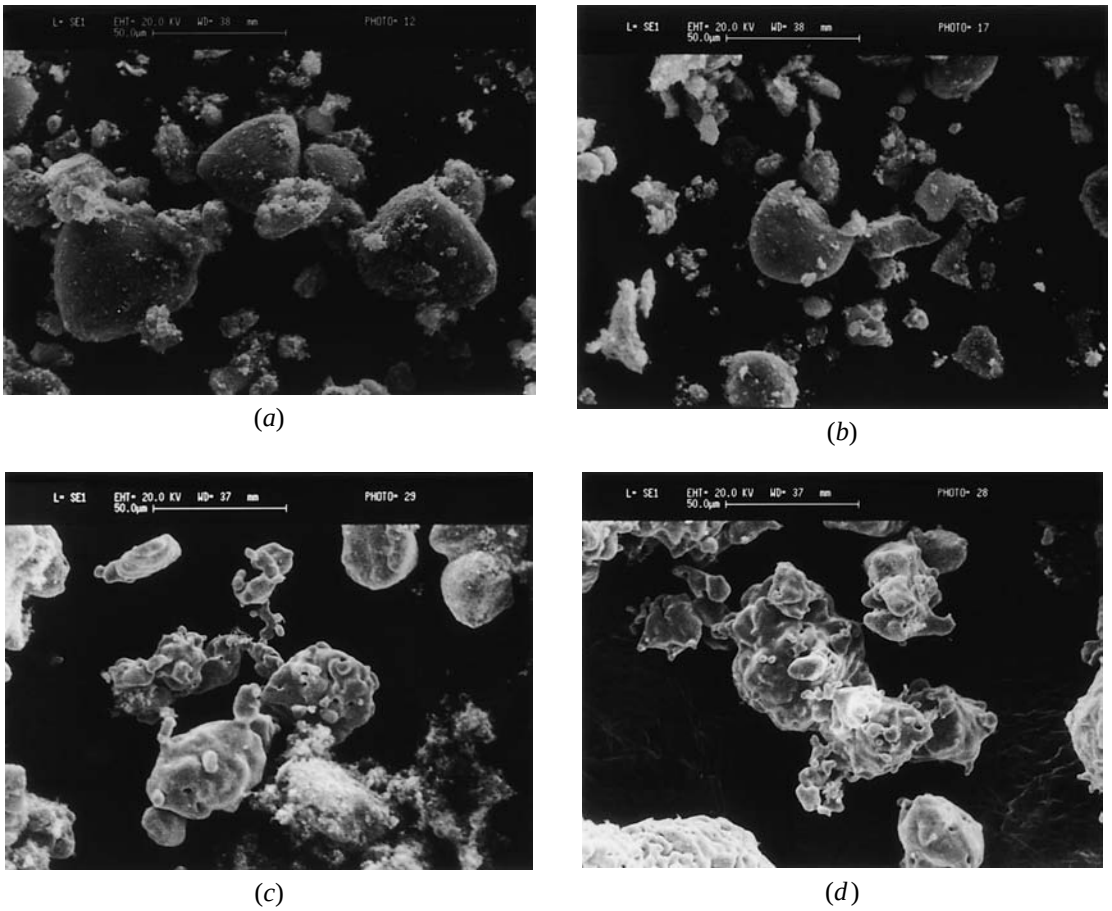

Fig. 5—SEM micrographs of solid samples. Reaction temperature = 1323 K: (*a*) unreacted, (*b*) 900 s, (*c*) 2250 s, and (*d*) 2700 s.

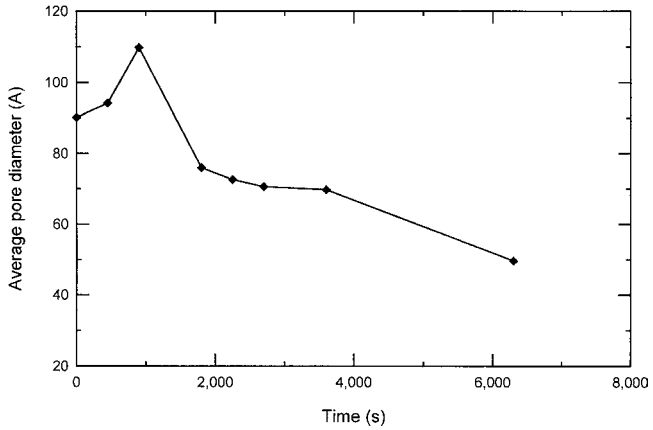

Fig. 6—Plot of average pore diamenter of partially reacted solid sample against reaction time. Reaction temperature = 1323 K.

of the pore diameter. Both increase as time increases, reach a maximum value at 900 seconds, and then decrease with a further increase in time. The following explanations can be given for these findings. The evaporation of Zn in the carbothemal reduction of ZnO in propagation stage I, Reaction [8], may generate small pores in the grains containing $ZnFe_2O_4$ (Figure 5(b)). The generation of pores increases the surface area of the specimen. In the propagation stage II, no additional evolution of Zn (g) occurs. Therefore, the rate of increase in the surface area is reduced. The escape of zinc vapor may also increase the pore volume and average pore diameter of the sample, initially. However, both drop after 900 seconds. The swelling of the solid caused by the crystallographic transformation, which occurs during the reduction of the iron oxides,[21] may be the reason for the suppression and the reduction of pore volume and pore size, respectively. From Figure 3, it can be observed that almost no more reaction occurs after 3600 seconds. Consequently, the pore volume and pore diameter are expected to be constant after this time. However, both of them drop after 3600 seconds. These contradictions are attributed to the sintering of the produced iron metal.

E. *General Discussion*

Based on the experimental results of the XRD, wet chemical analysis, SEM, and surface area meter, a model is proposed, as shown in Figure 7, in order to interpret the process of the carbothermal reduction of zinc ferrite.

Initially, at 0 to 450 seconds, $ZnFe_2O_4$ decomposes to ZnO and Fe_2O_3; the carbothermal reduction of ZnO and Fe_2O_3 proceeds; grains containing $ZnFe_2O_4$ become porous; the Boudouard reaction proceeds; and the size of the carbon grain diminishes.

Between 450 and 900 seconds, the reduction of ZnO and Fe_2O_3 continues; the surface area, pore volume, and average pore diameter increase rapidly; a reaction between CO_2 and C takes place; and the carbon grain shrinks.

When the reaction time reaches a range between 900 and

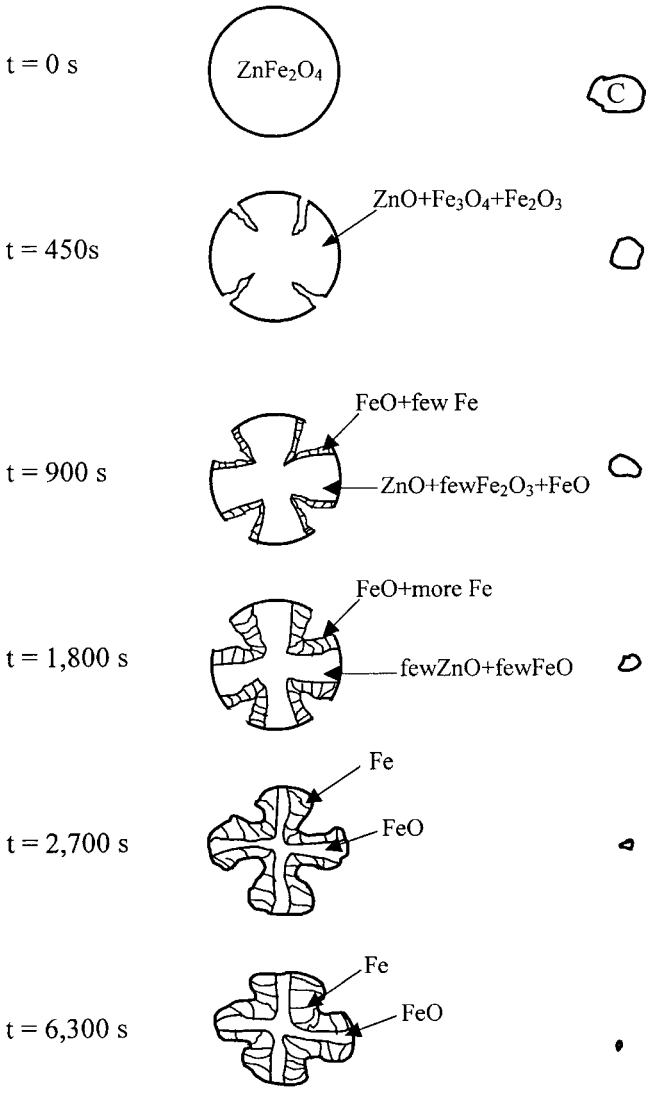

Fig. 7—Schematic representations of the variations of grains of $ZnFe_2O_4$ and C during reaction.

1800 seconds, the reduction rate of ZnO becomes low and the rate of increase in the surface area also lowers; the pore volume and average pore diameter reduce, due to the swelling of the grains containing $ZnFe_2O_4$; the Boudouard reaction continues; and the carbon grain size becomes very small.

In the range of 1800 to 2700 seconds, no additional reduction of ZnO occurs; the reductions of iron oxides slow down; the sintering of metal iron becomes predominant; the pore volume and pore diameter continue to drop; and the Boudouard reaction becomes slow.

At the final stage, from 2700 to 6300 seconds, no additional reactions occur, and the sintering of metal iron becomes significant. The pore volume and average pore diameter continue to drop.

F. *Effect of Argon Flow Rate*

The effect of the argon flow rate on the conversion of zinc ferrite is shown in Figure 8. It can be observed that the faster the gas flow, the faster the reaction takes place. The

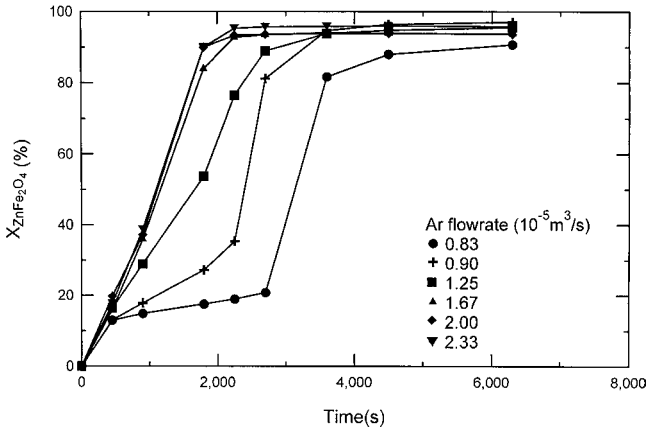

Fig. 8—Plot of conversion of $ZnFe_2O_4$ against time. Effect of Ar flow rate.

result can be explained as follows. Argon is a carrier gas and is not involved in the reaction. When the flow rate of argon is increased, the product gases of Reaction [1], *i.e.*, Zn (g) and CO (g) are easily removed from the solid matrix, and the conversion rate increases according to the calculations of Eqs. [3] and [4].

Liu *et al.*[16] carried out their reaction in a vacuum system and reported that the higher the degree of vacuum, the faster the degassing of zinc vapor occurs. It is thought that a higher degree of vacuum facilitates the escape of Zn (g) and CO (g) gases from the solid sample. Hence, the rate increases. Our results agree with theirs.

It is seen in Figure 8 that, at 1323 K with the sample height of 0.5×10^{-2} m, the mass transfer resistance in gas film can be ignored if the gas flow rate is higher than 2.00×10^{-5} m^3/s. Therefore, the flow rate of argon was kept at 2.33×10^{-5} m^3/s in all the experimental runs.

It is interesting to note that the reaction is very slow before 2700 seconds and increases rapidly after 2700 seconds for the flow rate of 0.83×10^{-5} m^3/s. The reason is that the metal iron produced by Reaction [11] or [15] catalyzed the Boudouard reaction, *i.e.*, Reaction [12] or [16].[22,23] Consequently, the overall rate of Reaction [1] is increased. Strictly speaking, the system should be considered as a noncatalyzed reaction in the initial stage and an iron catalyzed reaction in the later stage. The effect increases with the reaction time as the amount of the produced metal iron increases. As a result, for the experimental runs with higher flow rates, metal iron is produced earlier and it enters the stage of catalytic reaction earlier, as well.

G. *Effect of Sample Height*

The purpose of varying the sample height is to find out the ease with which the diffusion of Zn and CO occurs in solid sample. When the sample is high, the gases generated are not easy to diffuse out. Hence, it renders only a low conversion of zinc ferrite. The experimental results shown in Figure 9 agree with this expectation.

H. *Effect of Reaction Temperature*

Experiments were conducted at six different temperatures, in the range of 1073 to 1473 K; the results are shown in Figure 10. It can be seen that the increase in the reaction

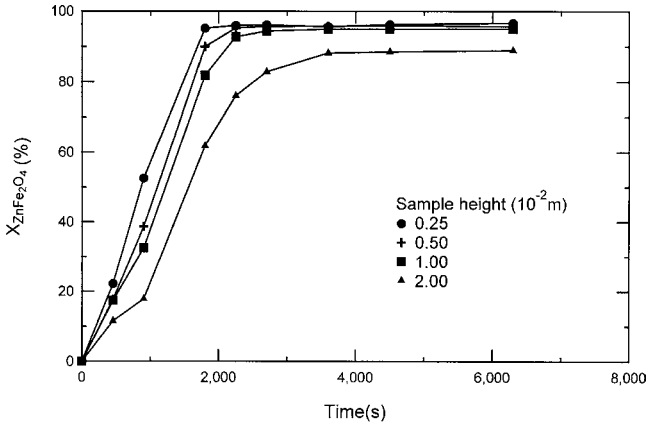

Fig. 9—Plot of conversion of $ZnFe_2O_4$ against time. Effect of sample height.

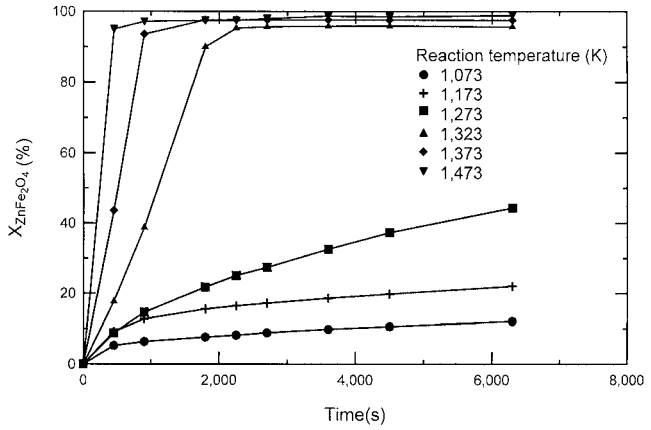

Fig. 10—Plot of conversion of $ZnFe_2O_4$ against time. Effect of reaction temperature.

temperature accelerates the reaction. Most investigators have reported similar results,[5–13] although their reactants are different from ours. When the reaction temperature is 1173 K, the conversion of zinc ferrite is only about 20 pct when the soaking time is over 6300 seconds. The reaction is speeded up greatly when the temperature is above 1323 K. The conversion of zinc ferrite reaches 95 pct at 1473 K for 450 seconds. Liu *et al.*[16] reported similar findings for the carbothermal reduction of EAF dust. To explain the big jump in reaction rate after 900 seconds from 1273 to 1323 K, one may suppose that much more iron is produced and that the catalytic effect of it on the Boudouard reaction is more powerful above 1273 K after 900 seconds, since this kind of acceleration has never before been found for the carbothermal reduction of ZnO.[6,8]

If the logarithmic value of the slope of the curve at $t = 0$ is plotted against the reciprocal value of the absolute temperature, an Arrhenius plot showing the temperature dependence of the initial rate is obtained; and is shown in Figure 11. The apparent activation energy obtained for the noncatalytic reaction was 92.91 kJ/mol. No previous report can be found concerning the activation energy values of the carbothermal reduction of zinc ferrite or EAF dust. However, the value for the reduction of zinc oxide was reported to be 148 and 356 kJ/mol by Zhang *et al.* (1989)[8] and Rao and Jalan (1977),[6] respectively.

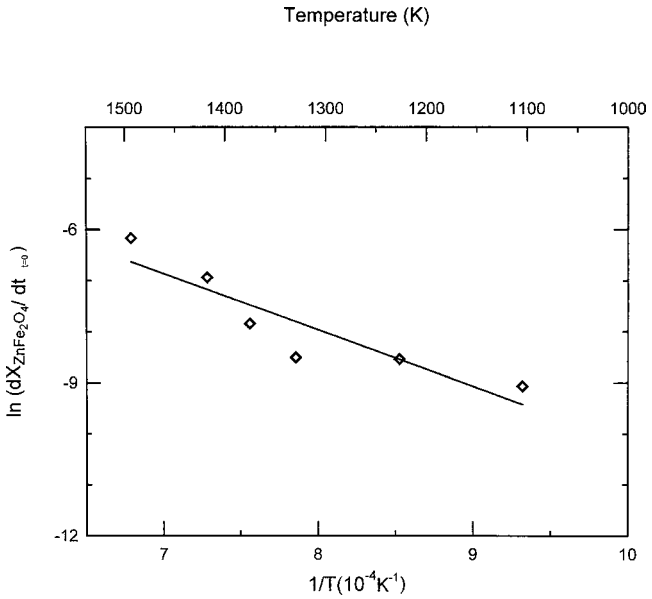

Fig. 11—Arrhenius plot showing the temperature dependency of the initial rate.

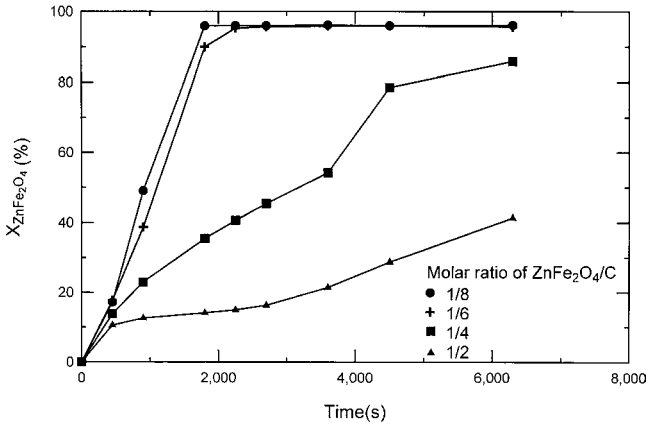

Fig. 12—Plot of conversion of $ZnFe_2O_4$ against time. Effect of molar ratio of $ZnFe_2O_4$/C.

I. *Effect of the Molar Ratio of $ZnFe_2O_4$/C*

The effect of the molar ratio of $ZnFe_2O_4$/C is depicted in Figure 12, which shows that the lower the molar ratio, the faster the reaction takes place. Furthermore, the effect is found to be heightened for the ratios higher than 1/6 and lowered for the ratios less than 1/6. When the ratio is low, more carbon is present in the solid sample, which accelerates the Boudouard reaction, as in Reaction [9] or [16]. Consequently, the overall reaction, Reaction [1], is enhanced. Although a high carbon content speeds up the process, the removal of the excess carbon after the reaction raises the production cost. Therefore, a compromise should be made to find out the optimal content of carbon in the solid sample.

One more interesting finding (Figure 12) is that inflection points between the noncatalytic and catalytic reaction still can be found in the experimental runs with the ratios of 1/2 and 1/4, since the reaction rates are low for these two runs.

J. *Effect of the Size of Carbon Agglomerate*

In this series of reactions, the grain size of zinc ferrite was kept constant as it was synthesized, at 62.61×10^{-6}

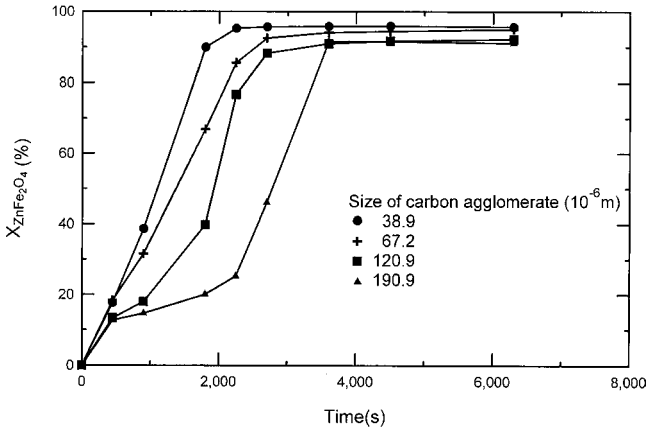

Fig. 13—Plot of conversion of $ZnFe_2O_4$ against time. Effect of size of carbon agglomerate.

m, while the size of the carbon agglomerate varied as 38.9×10^{-6} (350/400 mesh), 67.2×10^{-6} (200/300 mesh), 120.9×10^{-6} (120/140 mesh), and 190.9×10^{-6} m (60/100 mesh). It should be noted that the diameter of the carbon grain was found to be about 1×10^{-6} m and many agglomerates were found in the SEM micrographs in Figure 4(b). Hence, the size of the carbon in the range of 38.9 to 190.9×10^{-6} m should be that of the agglomerate instead of the grain itself. The corresponding results are shown in Figure 13, which indicates that the smaller the size of carbon agglomerate, the faster the reaction occurs. This is easy to understand, since the smaller size of the agglomerate facilitates the diffusion of CO_2 into the interior of the agglomerate to react with the carbon (Boudouard reaction, Reactions [12] and [16]). It results in the high rate of the overall Reaction [1].

Finally, it is also found that the inflection points appear in the curves of 120.9×10^{-6} and 190.9×10^{-6} m.

K. *Effect of Initial Bulk Density*

In this series of experiments, four experimental runs with different initial bulk densities, 785.9, 928.6, 1178.2, and 1375.6 kg m^{-3}, were carried out. The results, which are not shown here, indicate that when the initial bulk density is increased, the rate of reaction decreases. However, the influence is not significant. The results can be explained as follows. When the initial bulk density is high, the contact area between the zinc ferrite and carbon is large, which results in the high rate of Reaction [6]. However, a dense solid sample decreases porosity, which, in turn, hinders the escape of gases, zinc, and carbon monoxide. Hence, the reaction rate is decreased. The influence of the latter is stronger than that of the former such that reaction is slow when the initial bulk density is high and the effect is not significant. Present results agree with those of Liu *et al.* (1995).[16]

V. SUMMARY AND CONCLUSIONS

1. The $ZnFe_2O_4$ decomposes to ZnO and Fe_2O_3 initially, and carbothermal reductions of ZnO and Fe_2O_3 proceed simultaneously.
2. Initially, the evolution of zinc vapor makes grains containing $ZnFe_2O_4$ porous, which results in an increase in surface area, pore volume, and pore diameter.
3. The swelling of the solid during the reduction of iron oxides and the sintering of Fe reduces pore volume and pore diameter in the intermediate and later stages, respectively.
4. A mechanism and a model is proposed to interpret the overall reaction.
5. The overall rate of reaction can be increased by increasing the argon flow rate or reaction temperature. It can also be increased by decreasing the sample height, the molar ratio of $ZnFe_2O_4$/C, the size of the carbon agglomerate, or the initial bulk density.

ACKNOWLEDGMENTS

The authors thank the National Science Council of Taiwan for their financial support through Grant No. NSC-89-2214-E146-004. Thanks should also be extended to China Steel Corporation for the wet chemical analysis of the samples.

REFERENCES

1. H.S. Chang: *Taiwan 1999 Educational Programme on Waste Treatment of EAF Slag and Dust*, Taichung, Taiwan, Oct. 19–21, 1999, Taiwan Steel & Iron Industries Association, Taipei, Taiwan, 1999.
2. R. Kaltenhauser: *I & SM*, 1987, Mar., pp. 23-26.
3. C. Shi, J. Stegemann, and R. Caldrell: *Waste Management*, 1998, vol. 17 (4), pp. 249-55.
4. R.B. Ek and J.E. Schlobohm: *Iron Steel Eng.* 1993,
5. C.E. Guger and F.S. Manning: *Metall. Trans.*, 1971, vol. 2 (11), pp. 3083-90.
6. Y.K. Rao and B.P. Jalan: *TMS-CIM*, 1977, vol. 4, pp. 1-5.
7. Y.K. Rao: *J. Met.*, 1983, July, pp. 46-50.
8. C.F. Zhang, S. Rykichi, A. Iwazo, O. Osamu, and R.Q. Peng: *Metall. Rev. MMIJ*, 1989, vol. 6 (1), pp. 38-45.
9. H.K. Chen: Technical Report NSC88-2214-E-146-002, National Science Council of Taiwan, Taipei, Taiwan, 1999.
10. I.J. Lin and Y.K. Rao: *Inst. Mining Met. Trans.*, 1975, Sect. C, vol. 84, pp. c76-c82.
11. J.R. Donald and C.A. Pickles: *Metall. Mater. Trans. B*, 1996, vol. 27B, pp. 363-74.
12. R. Kola and H. Maczek: *Steel Times*, 1989, vol. 4, pp. 194-95.
13. J.C. Wang, M.T. Hepworth, and K.J. Reid: *J. Met.*, 1990, Apr., pp. 42-45.
14. F.A. Lopez, F. Medina, J. Medina, and M.A. Palacios: *Ironmaking and Steelmaking*, 1991, vol. 18 (4), pp. 292-95.
15. L. Wu and N.J. Themelis: *J. Met.*, 1992, Jan., pp. 35-38.
16. S.H. Liu, T.H. Hung, and S.T. Tsai: *Mining Metall.*, 1995, vol. 39 (4), pp. 109-19 (in Chinese).
17. J.R. Donald and C.A. Pickles: *Can. Metall. Q.*, 1996, vol. 35 (5), pp. 255-67.
18. Y.S. Kim and K.S. Han: *Proc. ROC-ROK Bilateral Workshop Mineral Beneficiation, Hydrometallurgy and Controls*, Nov. 24–29, 1980, Taipei, Taiwan, National Science Council of Taiwan, Taipei, Taiwan, 1980.
19. O. Kubaschewski, E.L. Evans, and C.B. Alock: *Metallurgical Thermochemistry*, Pergamon Press, Oxford, United Kingdom, 1993.
20. Y.K. Rao: *Chem. Eng. Sci.*, 1974, vol. 29, pp. 1435-45.
21. B.B.L. Seth and H.V. Ross: *Trans. AIME*, 1965, vol. 233, pp. 180-85.
22. G.R. Henning: *J. Inorg. Nucl. Chem.*, 1962, vol. 24, pp. 1129-36.
23. E.T. Turkdogan and I.V. Vinters: *Carbon*, 1972, vol. 10, pp. 97-111.